

## Characterization of Manganese doped ZnO (MZO) thin films by Spin Coating Technique

R. Mahendran<sup>1,2</sup>, M. Kashif<sup>3</sup>, T. Siva Kumar<sup>4</sup>, M. Saroja<sup>5</sup>, M. Venkatachalam<sup>5</sup>,  
A. Ayeshamariam<sup>6</sup>

<sup>1,2</sup>Department of Electronics, Government Arts College, Kulithalai, India

<sup>3</sup>Nano Biochip Research Group, Institute of Nano Electronic Engineering (INEE), Universiti Malaysia Perlis (UniMAP), Kangar 01000, Perlis, Malaysia

<sup>4</sup>Department of Electronics, RVS College of Arts and Science, Sulur, Coimbatore, India

<sup>5</sup>Thin Film Center, Department of Electronics, Erode Arts and Science College Erode, India.

<sup>6\*</sup>Department of Physics, Khadir Mohideen College, Adirampattinam 614 701, India

---

**Abstract:** Doping is a widely used to improve the structural and optical properties of semiconductors. However deposition route is also very important to get nanostructure with different properties. ZnO nanostructures doped with Mn having 5% doping concentrations by weight percentage have been synthesized in the laboratory using Spin coating technique. Scanning Electron Microscope (SEM) image shows the around one millimeter and X-ray diffractometer studies shows that the average diameter of the particles is 25 nm. From the UV-Vis studies the annealing temperature increases the crystal size decreases and the bandgap values increases accordingly.

**Keywords:** Crystal size, morphological studies, optical studies

---

### I. Introduction

Diluted magnetic semiconductors (DMS) have attracted much interest due to their potential application in Spintronics devices, such as spin-valve transistors, spin light-emitting diodes, non-volatile memory, logic devices, optical isolators and ultrafast optical switches [1]. In DMSs, transition metal doped II-VI and III-V semiconductors have been studied extensively [1]. One of the materials at the focus of much attention is the wide band gap wurtzite phase zinc oxide, a II-VI semiconductor, a well-known piezoelectric and electro-optic material with wide direct band gap (~3.37eV) and large exciton binding energy (60 meV) in which some of the zinc can be substituted by the manganese ions responsible for the ferromagnetic coupling [2,3]. ZnO doped with Mn has also been considered as an ideal material for short wavelength magneto-optical applications due to its wide band gap and the thermal solubility of Mn in ZnO [4]. Since the ionic radius of  $Mg^{2+}$  (0.57 Å) is similar to that of  $Zn^{2+}$  (0.60 Å), the latter can be substituted by the  $Mg^{2+}$  ion resulting in a wide range of solid solution [5].

However, the thermo dynamic solubility limit of MgO in ZnO is only about 4% as suggested by the phase diagram of MgO-ZnO binary system [6]. There are a number of reports on the growth of  $Mg_xZn_{1-x}O$  thin films using various techniques such as pulsed laser deposition (PLD) [7,8], laser ablation-molecular beam epitaxy (LA-MBE) [9], and radio frequency (rf) magnetron sputtering [10-11]. The substitution limit was found to be different for different techniques which are about 33% for PLD [12], 49% for molecular beam epitaxy (MBE) [13], and metal organic vapor phase epitaxy (MOVPE) [14]. Ohtomo et al. [15] have found that the thermodynamically MgO is soluble in  $Mg_xZn_{1-x}O$  up to a value of  $x = 0.15$ , while recently Ryoken et al. [16] reported the value to be in the composition range  $0.12 < x < 0.18$ . There are very few studies on the sol-gel  $Mg_xZn_{1-x}O$  thin films where substitution up to 20%, 33%, and 36% were reported [17-19]. Most of the reported work mainly correlates with the ferromagnetic properties of Mn-doped ZnO nanostructures and its origin. Thus, much work is needed to address the structural and optical properties of  $Zn_{1-x}Mn_xO$  owing to a growing interest of the magneto-optical effect. Pradhan et al. showed that  $Zn_{1-x}Mn_xO$  films grown at a substrate temperature of 500 °C exhibited room temperature ferromagnetism and beyond 500 °C the crystalline quality of the film increased at the expense of a decrease in the magnetization due to the formation of Mn related clusters [20]. Heo et al. studied the effect of post deposition annealing on the ferromagnetic properties of Mn implanted ZnO film deposited on sapphire substrate at 400 °C [21]. A significant enhancement in the magnetization of  $Zn_{1-x}Mn_xO$  film with an increase in annealing temperature (<600 °C) was observed and attributed to the improvement in crystalline quality [21]. The post deposition annealing treatment may lead to a more even distribution of substitutional  $Mn^{2+}$  and minimizing anti-ferromagnetic coupling in  $Zn_{1-x}Mn_xO$  thin films. [10]

## II. Experimental

Manganese-doped zinc oxide seed solution was prepared via a sol-gel spin-coating method. The Zn  $(\text{CH}_3\text{COO})_2 \cdot 2\text{H}_2\text{O}$ , and manganese acetate tetrahydrate  $(\text{Mn}(\text{OAc})_2 \cdot 2\text{H}_2\text{O})$ , were dissolved in 2-Methoxyethanol. Monoethanolamine (MEA) was added dropwise as a stabilizer under constant stirring. The concentration of ZnO was maintained at 1.0 M. The molar ratio of MEA to zinc acetate dehydrate was kept as 1:1 and the molar ratio of dopant manganese acetate tetra hydrate in the solution was 5 wt%. The solution was stirred at 70°C for 1 h. The precursor solution was dropped onto glass substrate which was rotated at 3000 rpm for 30 s. The films were dried at 300°C for 10 minutes in a furnace after each coating. The coating-to-drying process was repeated for 7 times. Finally, the films were annealed at 300°C – 450°C for 1 h. The ZnO film was white in appearance and Mn doped films were slightly brownish with a good adherence to the substrate.

The structural properties of the Mn doped ZnO thin films were investigated by recording the X-ray diffraction

(XRD) pattern using X-ray diffractometer (PANalytical X'Pert Pro) engaging Cu-K $\alpha$  radiation ( $\lambda = 1.54056 \text{ \AA}$ ). The surface morphology of the samples was investigated by scanning electron microscopy, SEM, (Hitachi S-3400N, Japan) and the chemical composition was examined using EDAX attachment (Nortan system six, Thermo electron corporation instrument, Super DRY 11, USA) with the SEM unit. For optical characterization, the transmission spectra of Mn doped ZnO thin films annealed at different temperatures were recorded using a UV-Vis spectrophotometer (Varian Cary 500 Scan). Varian Cary Eclipse spectrophotometer employing 15W Xe flash lamp was used for the photoluminescence studies.

The measured film thickness was approximately 0.53  $\mu\text{m}$  for doped film of RT and 0.51  $\mu\text{m}$ , 0.49, 0.46 and 0.41  $\mu\text{m}$  for Mn-doped films for different annealing. Thus the result clearly indicates that manganese incorporation promotes film growth rate with respect to temperature, this was measured by using Stylus Profilometer [22].

## III. Results And Discussion

### Structural Studies

Fig 1 shows the XRD patterns of 5 wt% Mn doped ZnO thin films prepared by sol-gel method and annealed at different temperature (300, 350, 400 and 450 C) with a fixed annealing time of 1 h. The XRD profiles, showing hexagonal wurtzite structure, were matched well with space group P63mc (36-1451) of wurtzite ZnO and no signatures of any impurity or binary zinc-manganese phase (including oxides of Mn and spinal phases) were observed. So the occurrence of impurity phases such as the oxides of Mn and spinal phase is ruled out in any of the doped samples. The texture coefficient of ZnO:Mn (MZO) thin films was estimated to determine the preferred orientation of polycrystalline thin films using the formula proposed by Barret and Massalski [23].

The XRD pattern reveals that the Mn doped films annealed at RT, 300°, 350° and 400° C displayed the amorphous natures, as the annealing temperature increases to 400 °C and 450 °C we get the crystalline nature and all the diffraction peaks are in accordance to the JCPDS card (36-1451) having the crystallite size of 29 and 14 nm, respectively. Apart from ZnO characteristic peaks, no extra peaks due to manganese clusters, zinc or their complex oxides could be detected. This observation suggests that the films are single phase and Mn ion might have substituted Zn site without changing the hexagonal structure.

Compared to pure ZnO film, the intensity of (101) peak slowly increases for Mn:ZnO (MZO) thin films. The (101) peak appears with maximum intensity in MZO at 450 °C with no preferred orientation [24].

Thus crystalline nature of films was affected due to enhancement of dopant concentration, by which manganese impurities were included in the ZnO crystal. Such loss of preferred orientation and crystalline nature with Mn incorporation has been reported by [25]. Mn doping with ZnO results in loss of preferred orientation along c-axis. In contrast, the substituted Mn ions at zinc sites deteriorated the host structure. Based on the ionic radius ( $\text{Zn}^{2+} = 0.60 \text{ \AA}$ ,  $\text{Al}^{3+} = 0.54 \text{ \AA}$  and  $\text{Mn}^{2+} = 0.66 \text{ \AA}$ ), the internal stress of MZO thin films is higher than AZO thin films because of the larger ionic radius of  $\text{Mn}^{2+}$ .

### Morphological Studies

#### SEM micrograph of MZO thin films at different temperatures

Fig 2 shows the SEM images of the 5 wt% Mn doped ZnO thin films annealed at different temperatures. It can be observed from figure 6 that the surface morphologies of the films changes greatly with an increase in annealing temperature. MZO thin films are possibly due to different expansion coefficients of ZnO, which increases the surface roughness of the thin films.

The scanning electron microscopy image of manganese-doped zinc oxide (MZO) thin films annealed at 300°, 350°, 400° and 450°C are shown in Fig. 2b, 2c, 2d and 2e. SEM images showed that annealing temperature has a vital function in controlling surface morphology. As shown in above figures, the film is assembled by the spherical nanoparticles that are distributed uniformly and monodispersity. The SEM analysis indicates that manganese-doped zinc oxide nanoparticles annealed at 450° C, having a granular surface. The film thickness

was also checked against cross-sectional SEM. Figs. 2a, 2b, 2c, 2d and 2e shows the cross-sectional SEM micrograph of Mn doped ZnO film of thickness varies from 0.40  $\mu\text{m}$  to 0.50  $\mu\text{m}$  measured by using Stylus Profilometer (obtained by 7 times coating).

The typical EDX spectrum of 5wt% Mn doped ZnO thin films is shown in Fig. 3, It exhibits the presence of Mn, though at lower atomic percentage as compared of the doping concentration. The EDX spectrum demonstrated the presence of zinc, oxygen, and magnese, which indicated the absence of any other impurities in the prepared sample. The EDX analysis showed that the amount of Mn incorporation increased with the increase in Mn concentration and also revealed the dominance of oxygen in all the samples exhibiting oxygen rich stoichiometry of thin films.

### Optical Studies of MZO thinfilms at different temperatures

#### UV-Studies

Fig. 3 and 4 shows the optical absorption and transmission spectra of MZO films in the visible range prepared under optimized conditions and annealed at various temperatures. The optical absorption and transmittance measurements are strongly dependent on annealing temperature, as shown in Fig 3 and 4. It can be notified from the figure as the annealing temperature increases, the transmittance of the MZO film increases gradually. Hence, the transmittance of the MZO thin films annealed at 400  $^{\circ}\text{C}$  and 450  $^{\circ}\text{C}$  are higher than 75% and 85% respectively, in the visible range.

A sharp decline in the transmittance of the UV region corresponds to the band gap. Fig 5 shows the optical band gap of the MZO thin films, respectively, estimated by extrapolation of the linear portion of  $(ahv)^2$  versus  $hv$  plots (Tauc's plot) using the relation  $ahv = A(hv - E_g)^2$ , where  $a$  is the absorption coefficient,  $hv$  the photon energy and  $E_g$  is the optical band gap. For different n values, a good linearity was observed at  $n = 1$  (direct allowed transition) which was found to give the best fit for these films. The optical band gap value gradually increases as the annealing temperature increased from RT to 450  $^{\circ}\text{C}$  of the SZO and AZO thin film has increased from 2.9 to 2.99eV.

It was observed that, with increasing annealing temperature of 5 wt% Mn doping band gap slightly increases but the grain size decreases. Impurity of Mn with ZnO band formation is an obvious consequence of increased annealing temperature [26] and the trapping of the Mn atoms at the grain boundary leads to the introduction of the Mn defect states within the forbidden band. With increasing Mn doping, density of this Mn induced defect states increases, leading to the observed slight increase of band gap or blue shift. Actually, trapping of Mn impurities within the grain and the introduction of Mn defect states within the forbidden band gap region is intimately related to the disorder introduced in the system by Mn doping. With decreasing grain size of 400  $^{\circ}\text{C}$  and 450  $^{\circ}\text{C}$  more and more disorder is introduced in the system.

#### PL Studies

Fig 6 shows room temperature photoluminescence (PL) spectra of Mn doped ZnO thin films on a glass substrate for different annealing temperatures. The little variation in PL intensities of all the films indicates a slight variation of film thicknesses due to annealing temperatures. The variation of film thickness is quite random and it has no direct correlation with Mn doping. In the PL spectra a UV emission peak centered at around ( $\sim 380$  nm) and a peak in the visible emission region with higher wavelength (410 nm) have been found. In the room temperature PL spectra of Mn doped ZnO thin film a dominant peak around ( $\sim 341$  nm or 3.60 eV and 343 nm 3.62) has been observed. The peak in the UV region corresponds to near band edge emission (NBE), because this peak is located close to the band gap energy ( $\sim 3.3$  eV), of ZnO at room temperature [27].

The UV emission is attributed to the radiative recombination of a hole in the valence band with an electron in the conduction band. It is quite remarkable that UV PL emission peak for all the doped and undoped films was broad and asymmetric in shape and bears a shoulder on the lower energy side. The origin of such an electron transition to shallow acceptor states [28], donor bound exciton transition [29] or combination of free exciton transition along with its phonon replicas [30] can be responsible for such broad transition. It has been observed that UV emission is stronger in undoped ZnO sample [31].

IV. Figures and Tables

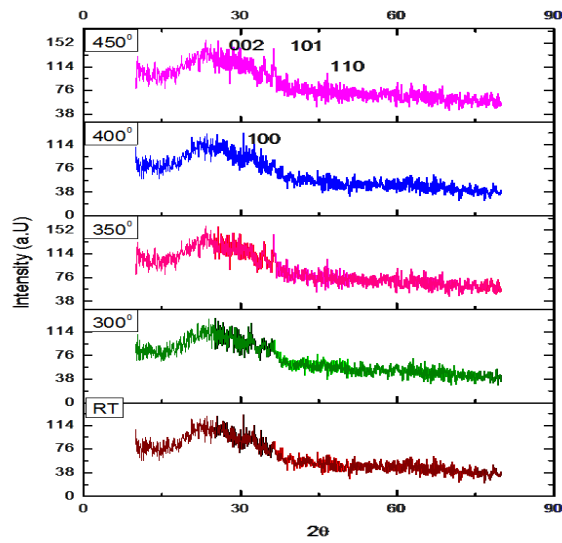


Fig 1 XRD pattern of Mn:ZnO (MZO) thin films at different annealing temperatures

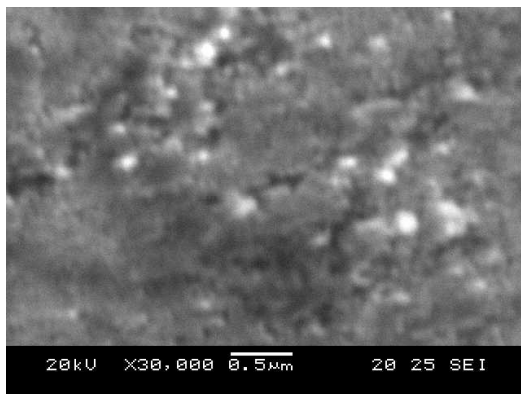


Fig2a XRD pattern of Mn:ZnO (MZO) thin films at RT

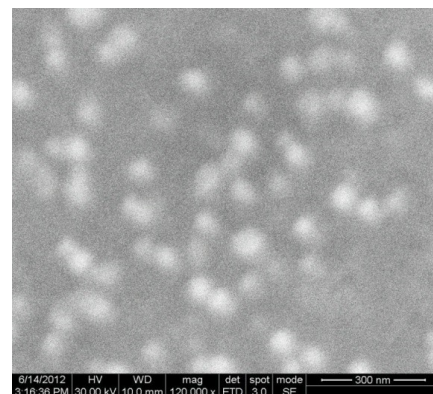


Fig2b XRD pattern of Mn:ZnO (MZO) thin films at 300° C

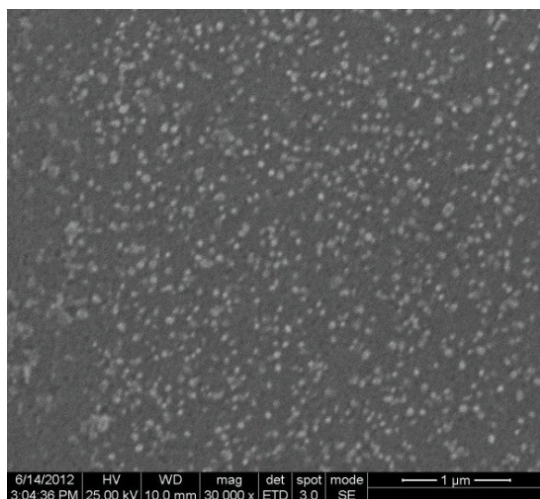


Fig 2c XRD pattern of Mn:ZnO (MZO) thin films at 350° C

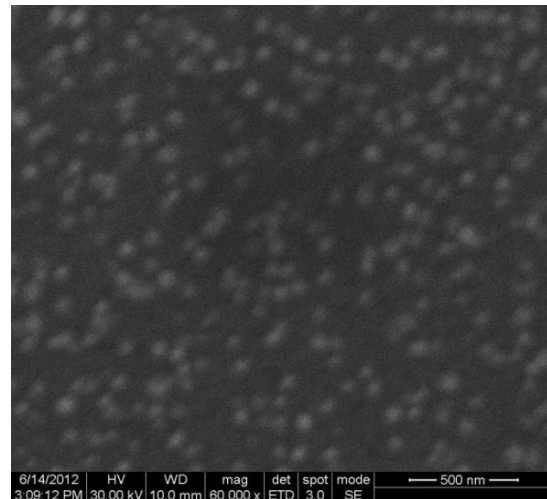


Fig 2d XRD pattern of Mn:ZnO (MZO) thin films at 400° C

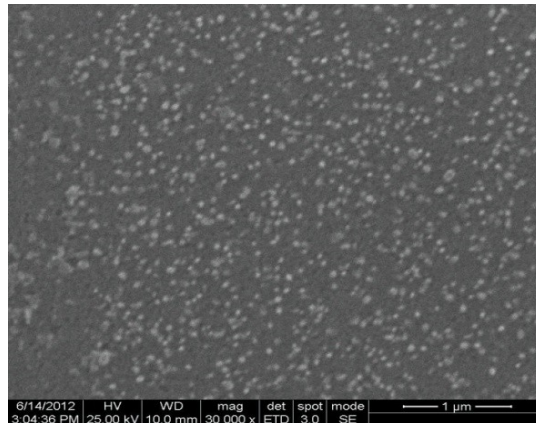


Fig 2e XRD pattern of Mn:ZnO (MZO) thin films at 450° C

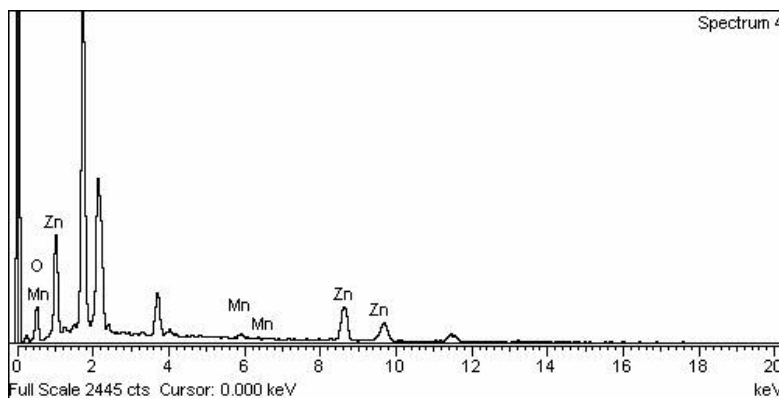


Fig 3 EDAX Analysis of MZO thin film at 450° C

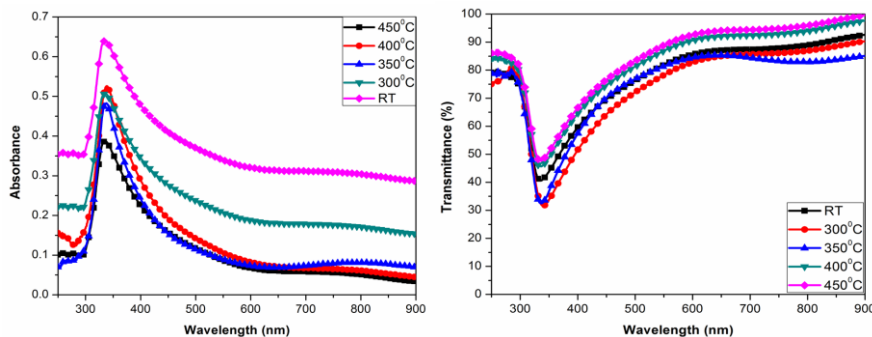


Fig 4 Absorbance curves of MZO thin film at different annealing temperatures  
Fig 5 Transmittance curves of MZO thin film at different annealing temperatures

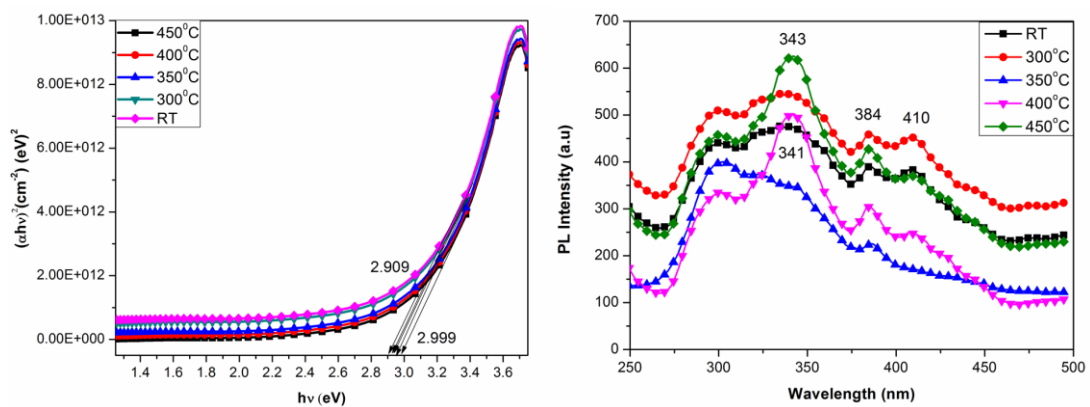


Fig .6 Optical band gaps of MZO thin films at different annealing temperatures.  
Fig. 7 Photoluminescence studies of MZO thin films at different annealing temperatures

Table .1 XRD Parameters Values of MZO thin films at different annealing temperatures.

Sample	FWHM	Particle size (nm)	Dislocation density $10^{15}$ lines/m <sup>2</sup>	Strain $10^{-3}$	Thickness of the film( $\mu$ m)
MZO RT	-	-	-	-	0.53
MZO 300 °C	-	-	-	-	0.51
MZO 350 °C	-	-	-	-	0.49
MZO 400 °C	0.33	29.1	1.18	1.245	0.46
MZO 450 °C	0.62	14.1	5.03	2.569	0.41

## V. Conclusion

The structural investigations were performed for MZO thin films of RT and annealed samples of different temperatures prepared by Spin Coating Technique. The optimized conditions are reported in Table 1.

The morphological analysis performed using SEM are reported. The studies agree to a great extent with the structural studies results. The undoped films with good electrical conducting grains and moderate grain size were chosen for further applications. The doping revealed a distinct microstructure in Mn doping. The morphological studies revealed excellent uniformity of the films. The compositional analysis performed using EDAX are reported. The studies agree to a great extent. The compositional analysis revealed slight metallic excess in the undoped samples irrespective of the concentration of the Zn ion in solution. The metallic excess is reduced when adding metallic salts in the solution. A competition for the metallic and nonmetallic sites is created in the solution when 'more metallic salts are present and the formation of series of solid solutions is not possible due to the Zn ions dominating the competition. A doping level of 5 wt% of atomic concentration is observed in Mn-doping.

The optical studies reveal that the MZO thin films are varying with respect to the annealed temperatures the band gaps from 2.9 eV to 2.99 eV. The films exhibited Moss-Burstein shift on doping. The PL spectra reveals that, MZO thin film exhibit the decrease in intensity of the band edge emission peak while the intensity of the deep level emission peak increases in the films coated on glass substrate. Doping is an effective approach to adjusting the Fermi energy level for semiconductors.

## References

- [1] Liu Y, Yang S-h, Zhang Y-l, Bao D-h. Influence of annealing temperature on structural, optical and magnetic properties of Mn-doped ZnO thin films prepared by sol-gel method. *Journal of Magnetism and Magnetic Materials*. 2009;321:3406-10
- [2] Kim KJ, Park YR. Spectroscopic ellipsometry study of optical transitions in  $Zn_{1-x}Co_xO$  alloys. *Applied Physics Letters*. 2002;81:1420-2.
- [3] Diaconu M, Schmidt H, Hochmuth H, Lorenz M, Benndorf G, Lenzner J, et al. UV optical properties of ferromagnetic Mn-doped ZnO thin films grown by PLD. *Thin Solid Films*. 2005;486:117-21.
- [4] Bates CH, White WB, Roy R. The solubility of transition metal oxides in zinc oxide and the reflectance spectra of  $Mn^{2+}$  and  $Fe^{2+}$  in tetrahedral fields. *Journal of Inorganic and Nuclear Chemistry*. 1966;28:397-405.
- [5] Shannon R. Revised effective ionic radii and systematic studies of interatomic distances in halides and chalcogenides. *Acta Crystallographica Section A*. 1976;32:751-67.
- [6] Segnit ER, Holland AE. The System MgO-ZnO-SiO<sub>2</sub>. *Journal of the American Ceramic Society*. 1965;48:409-13.
- [7] Sharma AK, Narayan J, Muth JF, Teng CW, Jin C, Kvit A, et al. Optical and structural properties of epitaxial  $Mg_xZn_{1-x}O$  alloys. *Applied Physics Letters*. 1999;75:3327-9.
- [8] Choopun S, Vispute RD, Yang W, Sharma RP, Venkatesan T, Shen H. Realization of band gap above 5.0 eV in metastable cubic-phase  $Mg_xZn_{1-x}O$  alloy films. *Applied Physics Letters*. 2002;80:1529-31.
- [9] Hayashi I, Panish MB, Foy PW, Sumski S. JUNCTION LASERS WHICH OPERATE CONTINUOUSLY AT ROOM TEMPERATURE. *Applied Physics Letters*. 1970;17:109-11.
- [10] Minemoto T, Negami T, Nishiwaki S, Takakura H, Hamakawa Y. Preparation of  $Zn_{1-x}Mg_xO$  films by radio frequency magnetron sputtering. *Thin Solid Films*. 2000;372:173-6.
- [11] Jia C-L, Wang K-M, Wang X-L, Zhang X-J, Lu F. Formation of c-axis oriented ZnO optical waveguides by radio-frequency magnetron sputtering. *Opt Express*. 2005;13:5093-9.
- [12] Ohtomo A, Kawasaki M, Koida T, Masubuchi K, Koinuma H, Sakurai Y, et al.  $Mg_xZn_{1-x}O$  as a II-VI widegap semiconductor alloy. *Applied Physics Letters*. 1998;72:2466-8.
- [13] Ohtomo A, Kawasaki M, Sakurai Y, Ohkubo I, Shiroki R, Yoshida Y, et al. Fabrication of alloys and superlattices based on ZnO towards ultraviolet laser. *Materials Science and Engineering: B*. 1998;56:263-6.
- [14] Park WI, Yi G-C, Jang HM. Metalorganicvapor-phase epitaxial growth and photoluminescent properties of  $Zn_{1-x}Mg_xO$  (0 <= x <= 0.49) thin films. *Applied Physics Letters*. 2001;79:2022-4.
- [15] Ohtomo A, Shiroki R, Ohkubo I, Koinuma H, Kawasaki M. Thermal stability of supersaturated  $Mg_xZn_{1-x}O$  alloy films and  $Mg_xZn_{1-x}O/ZnO$  heterointerfaces. *Applied Physics Letters*. 1999;75:4088-90.
- [16] Ryoken H, Ohashi N, Sakaguchi I, Adachi Y, Hishita S, Haneda H. Structures and properties of (Zn,Mg)O films studied from the aspect of phase equilibria. *Journal of Crystal Growth*. 2006;287:134-8.
- [17] Murakawa T, Fukudome T, Hayashi T, Isshiki H, Kimura T. Structural and optical properties of  $Mg_xZn_{1-x}O$  thin films formed by sol-gel method. *physica status solidi (c)*. 2004;1:2564-8.
- [18] Ji Z, Song Y, Xiang Y, Liu K, Wang C, Ye Z. Characterization of  $Mg_xZn_{1-x}O$  thin films prepared by sol-gel dip coating. *Journal of Crystal Growth*. 2004;265:537-40.
- [19] Zhao D, Liu Y, Shen D, Lu Y, Zhang J, Fan X. Photoluminescence properties of  $Mg_xZn_{1-x}O$  alloy thin films fabricated by the sol-gel deposition method. *Journal of Applied Physics*. 2001;90:5561-3.

- [20] Pradhan AK, Zhang K, Mohanty S, Dadson JB, Hunter D, Zhang J, et al. High-temperature ferromagnetism in pulsed-laser deposited epitaxial (Zn,Mn)O thin films: Effects of substrate temperature. *Applied Physics Letters*. 2005;86:152511.
- [21] Heo YW, Ivill MP, Ip K, Norton DP, Pearton SJ, Kelly JG, et al. Effects of high-dose Mn implantation into ZnO grown on sapphire. *Applied Physics Letters*. 2004;84:2292-4.
- [22] Mitra P, Khan J. Chemical deposition of ZnO films from ammonium zincate bath. *Materials Chemistry and Physics*. 2006;98:279-84.
- [23]. C. Barret, T.B. Massalski, *Structure of Metals*, Pergamon, Oxford, 1980.
- [24] Mitra P, Khan J. Chemical deposition of ZnO films from ammonium zincate bath. *Materials Chemistry and Physics*. 2006;98:279-84.
- [25] Nirmala M, Anukaliani A. Structural and optical properties of an undoped and Mn doped ZnO nanocrystalline thin film. *Photonics Letters of Poland*. 2010;2:189.
- [26] J. Pancove 'Optical Processes in Semiconductors', (1979) Prentice-Hall, EnglewoodCliffs, NJ.
- [27] Bandyopadhyay S, Paul GK, Sen SK. Study of optical properties of some sol-gel derived films of ZnO. *Solar Energy Materials and Solar Cells*. 2002;71:103-13.
- [28] Halperin BI, Lax M. Impurity-Band Tails in the High-Density Limit. I. Minimum Counting Methods. *Physical Review*. 1966;148:722-40.
- [29] Sieber B, Liu H, PiretGI, Laureyns J, Roussel P, Gelloz B, et al. Synthesis and Luminescence Properties of (N-Doped) ZnO Nanostructures from a Dimethylformamide Aqueous Solution. *The Journal of Physical Chemistry C*. 2009;113:13643-50.
- [30] Fonoberov VA, Alim KA, Balandin AA, Xiu F, Liu J. Photoluminescence investigation of the carrier recombination processes in ZnO quantum dots and nanocrystals. *Physical Review B*. 2006;73:165317.
- [31] Shan W, Walukiewicz W, Ager JW, III, Yu KM, Yuan HB, et al. Nature of room-temperature photoluminescence in ZnO. *Applied Physics Letters*. 2005;86:191911.